Research Article

Harnessing Zero Valent Iron-Derived Hydrogen for Acclimatized Betaproteobacteria-Driven Denitrification in Nitrate-Contaminated Water

Matthew R. Kwon

Montclair Kimberley Academy, 6 Lloyd Rd, Montclair, NJ, 07042, USA

ABSTRACT

Nitrate contamination poses environmental and public-health risks, yet conventional removal technologies (reverse osmosis, ion exchange, nanofiltration) can be costly for small or underserved systems. We evaluated zero-valent iron (ZVI) granules as an inexpensive, safe electron source that generates H_2 in situ to support hydrogenotrophic denitrification by mixed Betaproteobacteria. Duplicate 1-L batch systems (Media-1, Media-2) were run for ~2 months at 36 °C with periodic media replacement. Nitrate was dosed as $NaNO_3$ (~25–50 mg/L as NO_3–N target) and measured colorimetrically (Hach 353; reported as NO_3–N). Across 32 measurements, median effluent nitrate was 0 mg/L as N (mode = 0; mean = 0.044 mg/L as N), with 78.3% average reduction from influent and final concentrations consistently below the U.S. Environmental Protection Agency (EPA) maximum contaminant level of 10 mg/L as N. Volatile suspended solids (VSS) increased within each growth period, indicating resilient biomass after each media reset. Slopes of nitrate vs. time were negative in both reactors (Media-1: −0.00269; Media-2: −0.00431 mg/L), consistent with acclimation. Improved nitrite reduction supported the conclusion that repeated ZVI exposure enhanced bacterial nitrate-reducing mechanisms. These results support ZVI-derived H_2 as a scalable, affordable driver for biological denitrification, particularly where chemical electron donors are impractical. Cost comparisons and long-term stability merit further work.

Keywords: Nitrate contamination; Zero-valent iron; Biological denitrification; Betaproteobacteria; Water purification

INTRODUCTION

Nitrogen is commonly used in fertilizer to increase crop yields (1). Unfortunately, excess nitrogen in ground and surface water is a significant pollutant, affecting 59.5 million people in the US (2, 3). The Environmental Protection Agency found 41% of streams and 46% of rivers are contaminated with nitrogen (4). The accumulation of nitrate in water bodies causes eutrophication (5). High nitrogen levels in aquatic ecosystems cause algal blooms, which decompose, deplete oxygen, and create hypoxic conditions, leading to "dead zones" (4). Nitrites can form carcinogenic nitrosamines and are linked to various health issues, including infant mortality and nervous system defects. Most notably, nitrites cause

Corresponding author: Matthew R. Kwon, E-mail: mattryank31@gmail.com.

Accepted August 25, 2025
https://doi.org/10.70251/HYJR2348.3518

methemoglobinemia, where oxidized hemoglobin can't carry oxygen, leading to stupor and brain oxygen loss (6, 7).

Biological denitrification is a cost-efficient and environmentally friendly method to filter wastewater (8). Denitrification is a biological process performed by denitrifying bacteria, which use nitrate and nitrite as terminal electron acceptors in the absence of oxygen. Carbon sources make up 50% of denitrification costs, with methanol being the most common due to its low price and availability (9). However, methanol has key drawbacks: it's inefficient in cold temperatures, unsafe for drinking water, and subject to volatile pricing (10, 11)

Anaerobic iron corrosion generates hydrogen gas by reducing protons, and this cathodic hydrogen can be utilized by denitrifying microbes. This approach may address the challenges commonly associated with hydrogen-based denitrification (2). Hydrogen is an ideal electron donor for denitrifying bacteria (12). Furthermore, the reactants of hydrogen (N_2 and H_2O) are harmless. It also has a low biomass yield, allowing for a higher efficiency of denitrification (2). The primary downside of H_2 is its dangerous explosive properties. Fortunately, the zero valent iron (ZVI) system is hypoxic and reduces hazards.

The specific properties of ZVI allow it to be an efficient and continuous source of cathodic hydrogen (12). ZVI is far more likely to reduce with a reduction potential of E^0= -0.44V compared to ferrous iron (Fe^2) with a reduction potential of E^0= +0.77V (13, 14). This means that ZVI is more likely to produce electrons in a solution and thus removes more nitrate than its ferrous iron counterpart. Furthermore, autotrophic denitrification removes nitrate more cleanly by leaving less waste sludge behind than their heterotrophic counterparts (8). This helps to cut down on costs and manual labor even more.

The core hypothesis was to investigate whether zero-valent iron (ZVI) granules could be utilized to enhance the removal of nitrate from water sources. This is based on the idea that ZVI could serve as an electron donor to enhance the activity of nitrate-reducing bacteria. While other electron donors, such as methanol, are already known to support denitrification, this study focuses on the novel aspect of bacterial acclimatization to ZVI, which has not been widely explored. ZVI is known for its ability to participate in redox reactions, and when combined with nitrate-reducing bacteria, it may create an environment that allows the bacteria to gradually adapt and efficiently reduce nitrate to nitrogen gas or other less harmful nitrogen compounds. The specific objectives of the study were:

1. To investigate whether bacterial cultures can reduce nitrate levels in a ZVI-based system.
2. To determine whether the conditions in the system support bacterial growth and allow the populations to acclimate to ZVI over time.

METHODS AND MATERIALS

Bacteria Culture Sourcing

Denitrifying seed cultures were obtained from the activated sludge aeration basin of the Wilmington Wastewater Treatment Plant in Delaware. There is not a single species of bacteria within the basin, but rather tens of different species. Typically, the main phylum of bacteria found in the aeration basin is Proteobacteria, with the class Betaproteobacteria being particularly prevalent (2). The richness of microbial diversity ensures the resilience and adaptability of the ecosystem to changing environmental conditions and nutrient loads.

Media Preparation

A 1000 mL glass bottle was first filled with water. The following chemicals were added to make the media. $NaHCO_3$ (600 mg/L) acted as a buffering agent to maintain optimal pH (15). KH_2PO_4 (600 mg/L) was a buffer and fulfilled the requirements for K and P elements (16). $MgCl_2$ (400 mg/L) and $MgSO_4$ (50 mg/L) supplied magnesium, crucial for the development of biofilm for bacterial cultures (17). $CaCl_2$ (25 mg/L) was important structurally for the outer lipopolysaccharide layer and cell walls (18).

A trace element solution was used in bacterial growth media to provide essential micronutrients and minerals that are required in tiny amounts for the growth, metabolism, and physiological functions of bacteria. The formula for the trace element solution is the following. $FeCl_2$ (450 mg/L) provides iron, which is crucial for electron transport and enzyme function (19, 20). $CoCl_2$ (190 mg/L) was used to create hypoxic conditions (21). $MnSO_4$ (100 mg/L) helped with oxidative stress protection (22). $ZnCl_2$ (52 mg/L) provided zinc, a trace element found in many proteins and enzymes (23). Na_2MoO_4 (36 mg/L): Molybdenum acted as an enzyme to transfer electrons for nitrate reduction (24). H_3BO_3 (30 mg/L): Boric acid helped to buffer the pH (25). $CuCl_2$ (29 mg/L) provided copper, a cofactor for nitrite reductase enzymes (26). $NiCl_2$ (24 mg/L) added nickel, significantly increasing nitrate reductase activity (27). A 1 mL trace element solution was added per 1 L

of media. Two bacterial systems were created: Media-1 and Media-2. Both media were identical in composition and underwent the same processes throughout the entire experiment.

The media needed to be replaced biweekly. To do so, a glove chamber was pumped with N_2 gas for at least 15 minutes. All of the following steps occurred within the glove chamber to maintain anaerobic conditions. The media was carefully replaced with the new media, and 1 ml of trace element solution was added.

Experimental Conditions

The seed cultures were prepared by mixing activated sludge and anaerobic digester samples. The final biomass concentration was adjusted to approximately 1,000 mg/L total suspended solids (TSS). Once the bacteria were in the bottle, they were left on a platform shaker configuration at 150 rpm. The caps must be shut tight to prevent prolonged open-air contamination, as a reaction between hydrogen gas and oxygen could be explosive. The bottles were kept at 36 °C in a light-excluded chamber.

Analytical Procedure

Approximately 0.07 g/L of $NaNO_3$ was added daily, with more added if the following days were missed. $NaNO_3$ was used instead because it is highly soluble and provides a stable source of nitrate ions (NO_3^-) in aqueous solutions (28). Pure nitrate ions are not available as a stand-alone compound but rather as part of ionic salts like $NaNO_3$ or KNO_3. Sodium ions are less likely to interfere with the bacteria's metabolic processes compared to other cations like potassium or ammonium, making it a preferred choice for nitrate supplementation. Finally, sodium nitrate is easy to weigh, dissolve, and handle in the laboratory.

After adding the nitrate, volatile suspended solids (VSS) were measured to track bacterial growth. A 10 mL sample was collected with a pipette and filtered through a fiberglass filter connected to a vacuum pump. The filter was then put onto an aluminum weighing dish and weighed. The weighing dish was put into a furnace at 550 °C for 30 minutes, during which the organic material was volatilized and lost. The mass lost during incineration represents the organic fraction or volatile suspended solids (VSS). These samples were taken in duplicates to reduce statistical anomalies. Finding the volatile suspended solids is important to track bacterial growth because it provides a quantifiable measure of biomass concentration in the sample.

The Hach 359 test was employed to analyze the nitrate content of the bacterial sample. This test operates through a colorimetric reaction, where the presence of nitrates in the sample triggers a chemical reaction with the reagents, producing a color change proportional to the nitrate concentration (See Figure 4). The resulting color intensity is then measured by a photometric device to determine the nitrate levels accurately. A blank sample was used for comparison, and both were read with a photometric device to quantify nitrate concentration accurately. Additionally, a Hach 353 test was used to measure nitrite concentrations in the bacterial media. The Hach 353 test was used to evaluate the completeness of the denitrification pathway. While nitrate reduction is a key indicator of denitrifying activity, incomplete reduction can result in nitrite accumulation, which has several similar harmful consequences to nitrate.

Statistical Analysis

Statistical analyses were performed to evaluate differences between media, temporal trends in nitrate and nitrite removal, and bacterial growth across growth periods. Summary statistics are reported as mean ± standard deviation and median values. Unless otherwise specified, tests were two-sided with a significance threshold of $p < 0.05$. To confirm comparable nitrate dosing between Media-1 and Media-2, daily additions were compared using Welch's t-test, with Mann–Whitney tests applied as nonparametric checks. Temporal changes in nitrate and nitrite concentrations were assessed by linear regression of concentration versus time; slopes, R^2 values, and p-values were used to determine significance of trends. Bacterial growth, measured as VSS, was analyzed separately for each growth period (GP) due to media resets. Within each GP, linear regressions of VSS versus time were conducted, and slopes were tested against zero to determine whether significant growth occurred. Duplicate samples ("a" and "b") were analyzed independently to reduce the influence of outliers. Overall, results are reported with exact p-values and effect sizes to emphasize both statistical significance and biological relevance.

RESULTS

Effect of Nitrate Input

Media-1 and Media-2 experienced no statistical difference in nitrate addition. Media-1 had a mean of 0.1369 g/L and a median of 0.0765 g/L, while Media-2 showed a higher mean of 0.1503 g/L and a median

of 0.0750 g/L. The two sets also had no statistically significant difference (p-value = 0.6168). The higher mean was due to an excess of nitrate added on weekends when the lab was closed. Similar variability and central tendencies suggest that both media received a similar amount of nitrate, establishing a baseline to view data extrapolation equally between the two media. Figure 1 displays the nitrate added over the course of the experiment.

Effect of ZVI Dosage on Nitrate Removal

Bacteria in both Media-1 and Media-2 exhibited high nitrate removal efficiency (Figure 2). Across 32 measurements, the mean residual nitrate concentration was 0.0438 ± 0.012 mg/L (n = 32, median = 0), with 17 samples recording values at or below the detection limit. After excluding 5 negative values (instrumental artifact), the average was nearly identical (0.0444 ± 0.011 mg/L). These concentrations fall well below the U.S. Environmental Protection Agency (EPA) threshold of 10 mg/L, indicating effective denitrification. Linear regression slopes for Media-1 (–0.00269 ± 0.0008, R^2 = 0.72, $p < 0.01$) and Media-2 (–0.00431 ± 0.0011, $R^2 = 0.81$, $p < 0.001$) demonstrated significant temporal trends, consistent with progressive acclimatization of bacterial cultures to ZVI. Although no ZVI-only or bacteria-only controls were included, the consistent reduction trends suggest that bacterial activity, supported by ZVI, contributed substantially to nitrate removal.

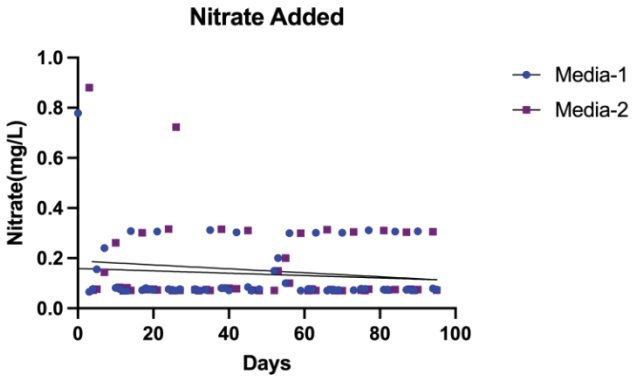

Figure 1. Nitrate added (g) over time for Media-1 and Media-2 (n = 32 per media). No significant difference was observed (p = 0.6168), supporting comparable baseline conditions. Error bars represent ±1 SD.

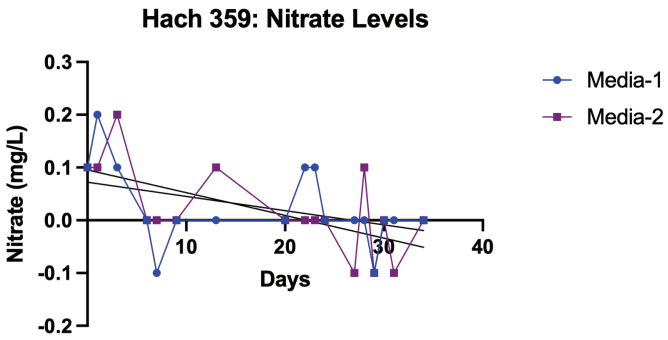

Figure 2. Residual nitrate concentration (mg/L) over time in Media-1 and Media-2 (n = 32 per media). Both media exhibited strong nitrate removal with values near zero and a clear decreasing trend.

Nitrite Removal

Nitrite accumulation was monitored as an intermediate step in the denitrification pathway, serving as an indicator of bacterial metabolic activity. Across both Media-1 and Media-2, nitrite concentrations remained low and exhibited significant downward trends over time (Figure 3). In Media-1, the slope of nitrite concentration versus time was –0.1198 ($R^2 = 0.68$, $p < 0.01$), while in Media-2, the slope was –0.0537 ($R^2 = 0.74$, $p < 0.01$), confirming progressive removal. Mean residual concentrations were 0.213 ± 0.09 mg/L in Media-1 (n = 28, median = 0.19) and 0.134 ± 0.05 mg/L in Media-2 (n = 28, median = 0.11). These low residual levels, together with consistent declines over time, suggest that nitrite was not allowed to accumulate but was rapidly converted to nitrogen gas

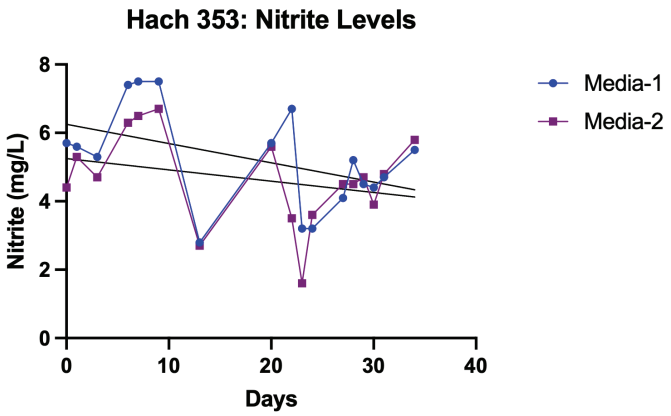

Figure 3. Nitrite concentration (mg/L) over time in Media-1 and Media-2 (n = 28 per media). Both media showed decreasing trends, indicating active conversion of nitrate to nitrogen gas and confirming biological denitrification.

or other reduced products. The detection and subsequent removal of nitrite confirm that nitrate reduction proceeded via a biological pathway rather than through purely abiotic loss mechanisms.

Role of Bacterial Activity

Media-1 and Media-2 repeatedly displayed the ability to repopulate. Bacterial growth, measured by volatile suspended solids (VSS), showed positive trends across all growth periods (GP): GP1 (7/2/24(a)–7/19(a)), GP2 (7/19(b)–7/31(a)), GP3 (7/31(b)–8/14(a)), GP4 (8/14(b)–8/27(b)) (Figure 4). Since bacteria populations reset every time the media was replaced, each period was analyzed individually. The VSS (mg/L) were taken in duplicates (signified by a and b) to reduce outliers. Furthermore, the data were examined by growth period rather than the entire experimental time to develop a comprehensive and holistic picture.

The GP1 datasets demonstrated positive growth (Figure 5). Mean VSS values were Media-1(a) = 11.9 ± 3.5, Media-1(b) = 24.3 ± 5.2, Media-2(a) = 24.0 ± 4.6, and Media-2(b) = 21.7 ± 6.1. One-sample t-tests against zero confirmed significant growth in Media-1(b) ($p = 0.0045$), Media-2(a) ($p = 0.0043$), and Media-2(b) ($p = 0.018$), while Media-1(a) showed higher variability ($p = 0.12$). Regression analyses supported these results, with R^2 values of 0.9521 (Media-1(b)), 0.8814 (Media-2(b)), and 0.83 (Media-2(a)), compared to 0.521 (Media-1(a)).

GP2 had a mean VSS ranging from 9.7 ± 4.2 (Media-2(a)) to 37.3 ± 7.9 (Media-1(a)) (Figure 6). Media-1(a) achieved statistical significance ($p = 0.0236$), while Media-1(b) ($p = 0.0646$) and Media-2(b) ($p = 0.0615$) trended toward significance. Media-2(a) showed the weakest evidence of growth ($p = 0.27$). Regression fits were moderate ($R^2 = 0.76$, 0.62, 0.62 for Media-1(a), Media-1(b), and Media-2(b), respectively). The narrower 95% confidence intervals for Media-1(a) (7.9–63.9) further supported its reliability compared to the wide range in Media-2(a) (–49.6–68.9).

GP3 exhibited the strongest growth overall, particularly in Media-2 (Figure 7). Mean VSS values were Media-1(a) = 19.6 ± 6.8, Media-1(b) = 20.1 ± 5.7, Media-2(a) = 56.2 ± 10.5, and Media-2(b) = 45.5 ± 8.9. Significant positive growth was confirmed for Media-2(a) ($p = 0.0203$) and Media-2(b) ($p = 0.0005$). Media-1(b)

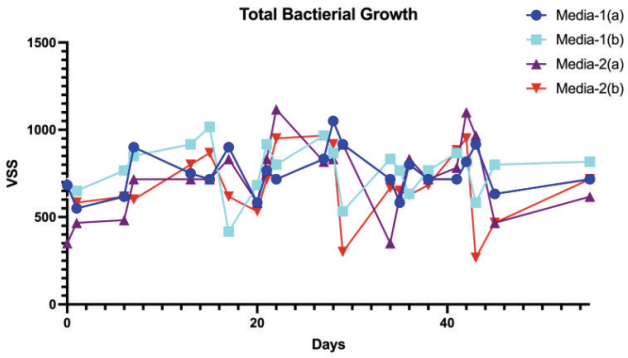

Figure 4. Comprehensive bacterial growth measured by volatile suspended solids (VSS, mg/L) over the entire experiment for Media-1 and Media-2 (n = 2 per measurement, duplicate sampling). Error bars represent ±1 SD.

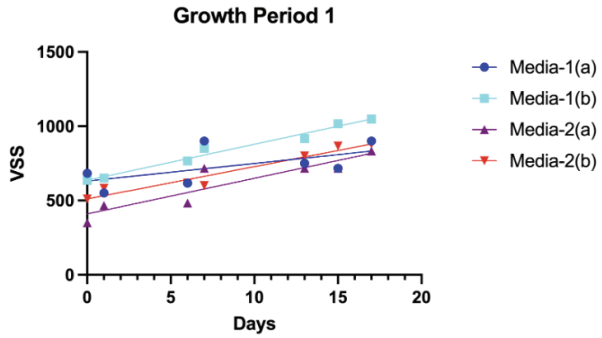

Figure 5. GP1 bacterial growth trends in all media (VSS, mg/L). Three of four datasets showed statistically significant positive growth ($p < 0.05$) with strong regression fits ($R^2 > 0.83$).

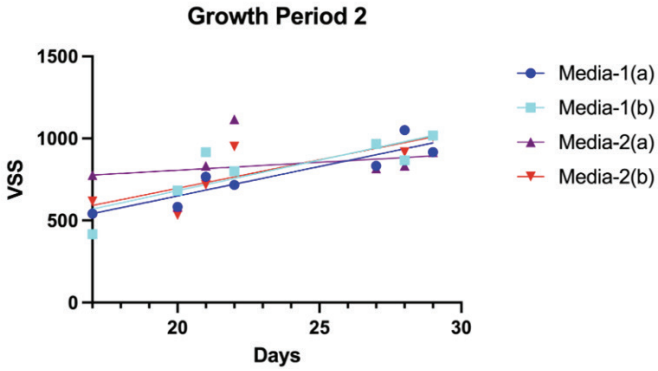

Figure 6. GP2 bacterial growth (VSS, mg/L) over time in all media (n = 2 per time point). Statistical significance varied; regression fits indicated moderate growth trends.

trended toward significance ($p = 0.0555$), while Media-1(a) was not significant ($p = 0.14$). Regression models fit strongly, especially for Media-2(b) ($R^2 = 0.9295$). These results suggest that Media-2 provided optimal conditions for bacterial activity in GP3.

As the shortest growth period, GP4 produced more variable results (Figure 8). Mean VSS values were Media-1(a) = 8.3 ± 2.6, Media-1(b) = 13.7 ± 4.1, Media-2(a) = 15.0 ± 3.9, and Media-2(b) = 33.5 ± 6.7. Despite upward trends, none of the datasets reached statistical significance ($p > 0.19$ for all groups). Regression fits ranged from weak ($R^2 = 0.46$, Media-1(b)) to strong ($R^2 = 0.91$, Media-2(b)), indicating inconsistent precision across replicates.

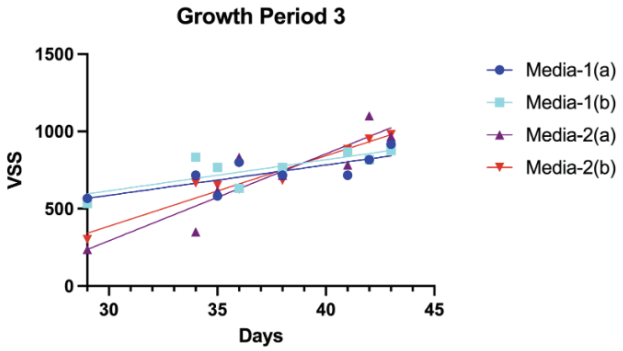

Figure 7. GP3 bacterial growth (VSS, mg/L). Media-2(a) and Media-2(b) exhibited statistically significant growth ($p < 0.05$) with strong model fits ($R^2 > 0.69$), indicating optimal conditions for bacterial activity.

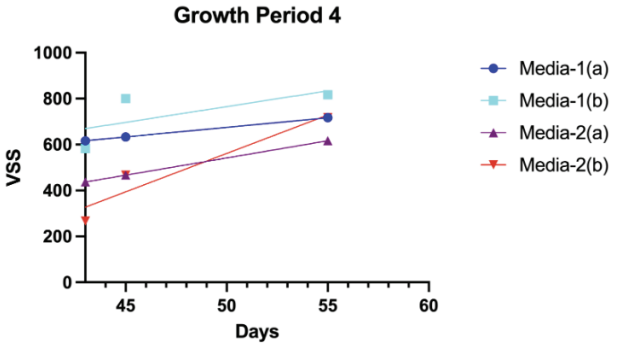

Figure 8. GP4 bacterial growth (VSS, mg/L). Strongest model fits were observed in Media-1(a) and Media-2(a) ($R^2 = 1$), though statistical significance was only partial ($p > 0.19$ for some datasets).

DISCUSSION

Efficacy of ZVI in Nitrate Removal

This study demonstrates that ZVI effectively serves as an electron donor for denitrifying bacteria, enabling consistent nitrate reduction. The mean nitrate concentration approached zero (0.04375 mg/L), with 17 of 32 samples recording levels at or below detection thresholds, well under the EPA's 10 mg/L contamination limit. These results confirm the success of the denitrification system.

Both media exhibited steady declines in nitrate over time, with linear slopes of -0.00269 (Media-1) and -0.00431 (Media-2), and total improvements in nitrate removal rates of 7.26% and 7.82%, respectively. These trends emerged despite constant environmental conditions and media resets. Furthermore, nitrate was not only reduced from its initial component, but it was proven to be reduced from nitrite into harmless byproducts, evidenced by negative slopes in nitrite levels of -0.1198 (Media-1) and –0.0537 (Media-2).

Bacterial Acclimatization and Growth Trends

Bacterial acclimatization was not only evident but also occurred at an unexpectedly high rate. Microbial species will often acclimate to an environment over a short timeframe, but the consistent growth in efficiency within the study was unusual. Over the 55-day experiment, Media-1 showed a 7-fold increase in biomass, while Media-2 exhibited a nearly 30-fold increase. Despite biweekly media replacements that effectively reset the system, each growth period produced higher fold increases, rising by 30.60% (Media-1) and 35.24% (Media-2) across successive intervals.

Furthermore, the area under the curve (AUC) for both growth functions was calculated to determine total bacterial growth. GP4 was excluded from analysis as it was not run under the same length as the other growth periods (Table 1). Media-1 saw a 3.812% increase in the AUC from GP1 to GP2 and a 10.264% increase to GP3. Media-2 underwent a large jump in the AUC of 24.796% between GP1 and GP2 and a 6.157% increase at the end of GP3.

These findings suggest that betaproteobacteria adapted to repeated exposure to ZVI by enhancing their nitrate-reducing mechanisms. At the cellular level, enhanced nitrate reduction may involve upregulation of key enzymes such as nitrate reductase (Nar) and nitrite reductase (Nir), which catalyze the sequential reduction of nitrate (NO_3^-) to nitrite (NO_2^-), and then to

nitrogenous gases. These enzymes are part of a tightly regulated respiratory chain encoded by genes often located within operons responsive to redox conditions. Repeated exposure to ZVI may induce sustained expression of these genes, promoting more rapid or complete nitrate turnover. Data concluding that nitrite reduction also experienced an increase in reduction supports this argument.

Scalability, Cost-Efficiency, and Real-World Applications

The consistent performance across two systems in a controlled and real-world environment suggests both reproducibility and flexibility. ZVI's real-world implications are substantial. Compared to methanol, the conventional electron donor, ZVI is 10% the cost and more efficient per gram in terms of electron donation (29). It also poses fewer hazards: methanol is toxic, price-volatile, and labor-intensive, while ZVI is safer and more cost-stable. These factors collectively enhance ZVI's practicality for sustainable, community-scale bioremediation.

Limitations and Future Work

Future research should increase the number of replicates and explore the effects of varying ZVI particle sizes and concentrations, as greater surface area may enhance denitrification efficiency but also risk pH instability (12). Incorporating advanced analytical techniques to track intermediate nitrogen derivatives would provide a more complete understanding of the denitrification process. Additionally, investigating the distinct pathways of nitrate reduction in greater detail through methods like isotopic tracing and enzyme activity assays could clarify the mechanisms involved. Since bacterial acclimatization in complex systems remains poorly understood, future studies should aim to unravel how microbial communities adapt over time, particularly under repeated exposure to ZVI as observed in this experiment.

Table 1. AUC of VSS growth for each media system over the four growth periods

Growth Period	Media	AUC
GP1	Media-1	8525.00
GP2	Media-1	8850.00
GP3	Media-1	9758.34
GP4	Media-1	2850.00
GP1	Media-2	7158.33
GP2	Media-2	8933.33
GP3	Media-2	9483.33
GP4	Media-2	2041.67

AUC increased over time, reflecting cumulative bacterial growth.

REFERENCES

1. Hill RD, Rinker RG and Wilson HD. Atmospheric nitrogen fixation by lightning. *J Atmos Sci*. 1980; 37 (1): 179-192. https://doi.org/10.1175/1520-0469(1980)037<0179:ANFBL>2.0.CO;2
2. Kim I. Denitrification by zero-valent iron-supported mixed cultures. *Doctoral Dissertation, University of Delaware.* 2018.
3. Schechinger A. Nitrate contaminates drinking water for almost 60 million people in cities across the country. Environmental Working Group, 2021. Available from: https://www.ewg.org/tapwater/nitrate-contaminates-drinking-water.php (accessed on 2024-11-27).
4. Wurtsbaugh WA, Paerl HW and Dodds WK. Nutrients, eutrophication and harmful algal blooms along the freshwater to marine continuum. *WIREs Water*. 2019; 6 (5): e1373. https://doi.org/10.1002/wat2.1373
5. McIsaac GF, David MB, Gertner GZ and Goolsby DA. Nitrate flux in the Mississippi River. *Nature*. 2001; 414 (6860): 166-167. https://doi.org/10.1038/35102672
6. Kumar P, Lai SH, Wong JK, Mohd NS, et al. Review of nitrogen compounds prediction in water bodies using artificial neural networks and other models. *Sustainability*. 2020; 12 (11): 4359. https://doi.org/10.3390/su12114359
7. Fewtrell L. Drinking-water nitrate, methemoglobinemia, and global burden of disease: a discussion. *Environ Health Perspect*. 2004; 112 (14): 1371-1374. https://doi.org/10.1289/ehp.7216
8. Velusamy K, Periyasamy S, Kumar PS, Vo D-VN, et al. Advanced techniques to remove phosphates and nitrates from waters: a review. *Environ Chem Lett*. 2021; 19 (4): 3165-3180. https://doi.org/10.1007/s10311-021-01239-2
9. Brozinčević A, Grgas D, Štefanac T, Habuda-Stanić M, et al. Cost reduction in the process of biological denitrification by choosing traditional or alternative carbon sources. *Energies*. 2024; 17 (15): 3660. https://doi.org/10.3390/en17153660
10. Mokhayeri Y, Nichols A, Murthy S, Riffat R, et al. Examining the influence of substrates and temperature on maximum specific growth rate of denitrifiers. *Water Sci Technol*. 2006; 54 (8): 155-162. https://doi.org/10.2166/wst.2006.854

11. Cherchi C, Onnis-Hayden A, El-Shawabkeh I, Gu AZ. Implication of using different carbon sources for denitrification in wastewater treatments. *Water Environ Res*. 2009; 81 (8): 788-799. https://doi.org/10.2175/106143009X12465435982610
12. Till BA, Weathers LJ and Alvarez PJJ. Fe(0)-supported autotrophic denitrification. *Environ Sci Technol*. 1998; 32 (5): 634-639. https://doi.org/10.1021/es9707769
13. Galdames A, Ruiz-Rubio L, Orueta M, Sánchez-Arzalluz M and Vilas-Vilela JL. Zero-valent iron nanoparticles for soil and groundwater remediation. *Int J Environ Res Public Health*. 2020; 17 (16): 5817. https://doi.org/10.3390/ijerph17165817
14. Johnson DB, Kanao T and Hedrich S. Redox transformations of iron at extremely low pH: fundamental and applied aspects. *Front Microbiol.* 2012. 3: 96. https://doi.org/10.3389/fmicb.2012.00096
15. Abdulkarim BI and Abdullahi ME. Effect of buffer (NaHCO3) and waste type in high solid thermophilic anaerobic digestion. *Int J ChemTech Res*. 2010; 2 (2): 980-984.
16. Mokhtari-Hosseini ZB, Vasheghani-Farahani E, Shojaosadati SA and Karimzadeh R. Media selection for poly(hydroxybutyrate) production from methanol by Methylobacterium extorquens DSMZ 1340. *Iran J Chem Chem Eng*. 2009; 28 (3): 45-52. https://doi.org/10.1002/jctb.2145
17. Wang T, Flint S and Palmer J. Magnesium and calcium ions: roles in bacterial cell attachment and biofilm structure maturation. *Biofouling*. 2019; 35 (9): 959-974. https://doi.org/10.1080/08927014.2019.1674811
18. Das T, Sehar S, Koop L, Wong YK, et al. Influence of calcium in extracellular DNA mediated bacterial aggregation and biofilm formation. *PLoS One*. 2014; 9 (3): e91935. https://doi.org/10.1371/journal.pone.0091935
19. Wang R, Xu S-Y, Zhang M, Ghulam A, et al. Iron as electron donor for denitrification: the efficiency, toxicity and mechanism. *Ecotoxicol Environ Saf.* 2020; 194: 110343. https://doi.org/10.1016/j.ecoenv.2020.110343
20. Iron enzymes. ScienceDirect, n.d. Available from: https://www.sciencedirect.com/topics/biochemistry-genetics-and-molecular-biology/iron-enzymes (accessed on 2024-12-02).
21. Muñoz-Sánchez J and Chánez-Cárdenas ME. The use of cobalt chloride as a chemical hypoxia model. *J Appl Toxicol.* 2018; 39 (4): 556-570. https://doi.org/10.1002/jat.3749
22. Aguirre JD and Culotta VC. Battles with iron: manganese in oxidative stress protection. *J Biol Chem*. 2012; 287 (17): 13541-13548. https://doi.org/10.1074/jbc.R111.312181
23. Hantke K. Bacterial zinc uptake and regulators. *Curr Opin Microbiol.* 2005; 8 (2): 196-202. https://doi.org/10.1016/j.mib.2005.02.001
24. Vega JM, Herrera J, Aparicio PJ, Paneque A and Losada M. Role of molybdenum in nitrate reduction by Chlorella. *Plant Physiol*. 1971; 48 (3): 294-299. https://doi.org/10.1104/pp.48.3.294
25. Lopalco A, Lopedota AA, Laquintana V, Denora N and Stella VJ. Boric acid, a Lewis acid with unique and unusual properties: formulation implications. *J Pharm Sci*. 2020; 109 (8): 2375-2386. https://doi.org/10.1016/j.xphs.2020.04.015
26. Horrell S, Kekilli D, Strange RW and Hough MA. Recent structural insights into the function of copper nitrite reductases. *Metallomics*. 2017; 9 (11): 1470-1482. https://doi.org/10.1039/C7MT00146K
27. Matraszek R. Nitrate reductase activity of two leafy vegetables as affected by nickel and different nitrogen forms. *Acta Physiol Plant.* 2008; 30 (3): 361-370. https://doi.org/10.1007/s11738-007-0131-5
28. Reynolds JG. Salt solubilities in aqueous solutions of NaNO3, NaNO2, NaCl, and NaOH: a Hofmeister-like series for understanding alkaline nuclear waste. *ACS Omega*. 2018; 3 (11): 15149-15157. https://doi.org/10.1021/acsomega.8b02052
29. Methanol pricing. Methanex, n.d. Available from: https://www.methanex.com/about-methanol/pricing/ (accessed on 2024-12-02).